Simplification of Mannequin Based on Fuzzy Partition of Geometric Information Gain Metric

Ye Yuan[1] Qing-Fu Li[2]

[1] School of Information Engineering, Beijing Institute of Fashion Technology

Beijing 10029, Beijing, China

colayuan@163.com

[2] Department of Elements, Beijing Institute of Fashion Technology

Beijing 10029, Beijing, China

jcblqf@bift.edu.cn

Received 1 March 2015; Revised 6 April 2015; Accepted 16 April 2015

Abstract. Focusing on the maintenance of important shape features during the mannequin simplification process, a new simplification method, driven by fuzzy partition of geometric information gain metric is proposed in this paper. The integration of distance, non-planarity, change of the normal has been defined as the geometric information gain metric to measure the geometric information content of each vertex. The geometric information gain metric is subsequently partitioned into three fuzzy sets to indicate the weak, moderate and strong geometry salience of vertices on the underlying mannequin in which thresholding values for fuzzy sets are selected by minimum fuzziness degree principle. The resulted fuzzy sets of geometric information gain metric are then introduced to the edge collapse operation to determine the vertices incident to candidate edges for contraction. The proposed approach is capable of reducing simplification error and maintaining mannequin's feature dimensions as well. Simulation results show that the new algorithm facilitate better approximations with regard to both visual fidelity and geometric errors than Garland's quadric error metric algorithm.

Keywords: simplification of mannequin, fuzzy partition, geometric information gain metric

1 Introduction

With the emergence of new 3D scanning techniques [1-4], detailed geometric mannequins acquired at a very high resolution are widely applied to many fields such as industry, arts and military. Models produced by the 3D scan data can often be very densly organized meshes with increasing complexity and computational times. However, details of the reconstructed model actually vary considerably due to various acquisition and fitting schemes. A highly complex model capturing very fine surface details is not always necessary for applications. For the instance of garment pattern generation, the surface geometry of a 3D garment protype is directly related to the individual human body sizes. In all these applications, there exists a compromise between the accuracy and computational efficiency. Simplification of surface meshes is an essential approach to trim large scale data of the mannequin to satisfy individual application requirements.

Up to now, many contributions have been made to this field. Currently used object simplification methods are roughly categorized into vertex clustering [5-7], region merging, mesh retiling, geometric primitives decimation, and progressive refinement .

Vertex clustering methods exploit geometric proximity [5] to group object vertices into clusters, and then replace each cluster by a newly computed vertex, which is followed by a retriangulation process for all newly generated vertices. Since the position of a new vertex is calcuated using simple weighted mean regarding vertices within each cluster, it is incaple of maintaining topological structures of the object. To alleviate the disadvantages of vertex clustering, Importance degree [6] is associated with each vertex, by which a floating-cell clustering operation is proceeded, while in [7] a 3D grid clustering technique together with quadric error metric is presented to deal with simplifying very large scale object.

Region merging is conducted by combining the selected seed facet with its neighbouring facets satisfying given criterion (e.g. coplanarity) to form a superfacet, and then by retriangulating the superfacet into fewer facets than those of the original object [8]. Region partition [9], facets grouping with coincident normals [10] , and simplification envelopes [11] are alternatives to cope with emerging holes and high computational cost resulted by conventional region merging algorithms.

Mesh retiling methods [12] are characterized by a number of sequential operations such as randomly distributing a new set of vertices over the initial object surface, retiling an intermediate mesh through connecting these newly inserted vertices one another, removing each another, removing each original vertex, and finally re-triangulating the surface in a way that matches the local geometry and topology of the initial surface. A well-established extension [13, 14] to mesh retiling methods is implemented by transforming the polygonal geometry into a 3D grid of voxels, to which a low pass filtering operation is subsequently applied for the removal of high frequency details.

Guided by one of the decimation error measures such as geometry criteria [15-17], information-theoretic measure [18-20], visual similarity [21, 22] and saliency metric [23-25], geometric primitives decimation methods operate on iteratively eliminating the constructional elements, i.e. vertices, edges and triangles .

In the case of vertex elimination [26, 27], multiple passes are exploited over all vertices on the object surface. Those vertices satisfying a user-specified distance or angle criterion and all incidental triangles are progressively deleted, which is followed by a local re-triangulation process to fill the resulting holes. In the other cases, the simplification of a mesh is achieved either by iteratively collapsing edges into vertices [28, 29] or by collapsing triangles into vertices [17].

Progressive refinement methods are constructed by two sequences of dual mesh transformation, which are edge collapse and vertex split [30, 31]. As a result of successive edge collapse transformations, a base mesh is the most simplified version in approximating the initial object. However, a sequence of vertex split transformations applied progressively to the base mesh result in a level-of-detail (LOD) representation of the initial object.

Despite the high computational efficiency and capability to simplify non-manifold meshes, vertex clustering methods are incapable of preserving topology and small-scale details of the original meshes. Although the facets merging process is topology tolerant and simplification maneuverable, it suffers from heuristic criteria, which result in unnencessarily optimal superfacets. Additionally, there probably exists holes in the face merging regions. Retiling approaches can present good simplification results on smooth surfaces. However, the accuracy and conciseness of the resulted meshes are counterbalanced to some extent by substantial processing times. quadric error metrics [32] are devised to guide the simplifying process by iteractively contracting arbitrary vertex pairs, which possess efficiency, quality and generality. Since this scheme depends merely on the sum of squared distances of each vertex to its incident triangle planes disregarding local geometry and topology, it accordingly has exhibited limitations to the quality of geometric fidelity of simplified results.

To attenuate the disadvantages of Garland's quadric error metric, geometric information gain metric is proposed in this paper to measure the local geometry corresponding to each vertex, which are fuzzily partitioned into three priority sets. All edges to be collapsed are determined by priorities of the geometric information gain of associated vertices.

2 Definition of the Geometric Information Gain

The definition of geometric information gain corresponding to every vertex of the object is dependent on the distance measure, the non-planarity measure, and the normal variation measure of the object's surface. Let $\boldsymbol{V}_j = \boldsymbol{V}_i + \boldsymbol{\delta}_{ij}$ for $j = 1, 2, \cdots, k$ be the neighbours of $\boldsymbol{V}_i$. Suppose that $\boldsymbol{n}_j$ and $\boldsymbol{n}_i$ are the respective normal directions of $\boldsymbol{V}_j$ and $\boldsymbol{V}_i$, which can be evaluated by averaging the normal vectors of the neighboring triangular meshes. Borrowing some notions from [33] , the distance measure $G_d(\boldsymbol{V}_i)$ (Ref. Fig.1 (a))) is given by.

$$G_d(\boldsymbol{V}_i) = \left\| \boldsymbol{V}_j - \boldsymbol{V}_i \right\|_2^2 = \left\| \boldsymbol{\delta}_{ij} \right\|_2^2 = \sum_{j=1}^{k} \sigma_{ij}^2 \quad , \tag{1}$$

where $\boldsymbol{\delta}_{ij} = \left(\sigma_{i1}, \sigma_{i2}, \cdots, \sigma_{ik} \right)^T$. Then the non-planarity measure $G_p\left(\boldsymbol{V}_i\right)$ (Ref. Fig. 1 (b)) is formulated as

$$G_p\left(\boldsymbol{V}_i\right) = \sum_{j=1}^{k} \left(\boldsymbol{n}_i^T \boldsymbol{\delta}_{ij} \right)^2 . \tag{2}$$

And then the normal variation measure $G_c\left(\boldsymbol{V}_i\right)$ (Ref. Fig. 1 (c)) is represented by

$$G_c\left(\boldsymbol{V}_i\right) = \sum_{j=1}^{k} \left\| \boldsymbol{n}_i - \boldsymbol{n}_j \right\|_2^2 \cdot \sigma , \tag{3}$$

where $\sigma = \frac{1}{k} \sum_{j=1}^{k} \sigma_{ij}^2$. Performing normalization on the distance measure $G_d(\boldsymbol{V}_i)$, the non-planarity measure $G_p\left(\boldsymbol{V}_i\right)$, and the normal variation measure $G_c\left(\boldsymbol{V}_i\right)$ results in

$$g_d(\boldsymbol{V}_i)=\frac{G_d(\boldsymbol{V}_i)-\min\left(G_d(\boldsymbol{V}_i)\right)}{\max\left(G_d(\boldsymbol{V}_i)\right)-\min\left(G_d(\boldsymbol{V}_i)\right)}, \tag{4}$$

$$g_p(\boldsymbol{V}_i)=\frac{G_p(\boldsymbol{V}_i)-\min\left(G_p(\boldsymbol{V}_i)\right)}{\max\left(G_p(\boldsymbol{V}_i)\right)-\min\left(G_p(\boldsymbol{V}_i)\right)}, \tag{5}$$

and

$$g_c(\boldsymbol{V}_i)=\frac{G_c(\boldsymbol{V}_i)-\min\left(G_c(\boldsymbol{V}_i)\right)}{\max\left(G_c(\boldsymbol{V}_i)\right)-\min\left(G_c(\boldsymbol{V}_i)\right)}. \tag{6}$$

The definition of geometric information gain with respect to vertex $\boldsymbol{V}_i$ is hereby followed by

$$g_i=\lambda_c g_c(\boldsymbol{V}_i)\left[\lambda_d g_d(\boldsymbol{V}_i)+\lambda_p g_p(\boldsymbol{V}_i)\right], \tag{7}$$

where coefficients λ_d, λ_p and λ_c are assigned 0.3, 0.3, 0.4 respectively satisfying $\lambda_c+\lambda_d+\lambda_p=1$. In the definition of geometric information gain, the normal variation measure is a dominant factor to provide every vertex with a significant geometry information content increment. Provided there is normal deviation between two vertices, local shapes of their incidental facets are much less similar to each other. Consequently, the normal variation measure is established to be the multiplier in (7). However, the individual contribution of the distance measure and the non-planarity measure to the geometric information gain is small relatively. The sum of the distance measure and the non-planarity measure is accordingly set to be the other multiplier.

Due to the accessibility of the geometric information gain of mannequin at a given vertex, the diverse values of geometric information gain can provide us with an approach to guide the simplification process

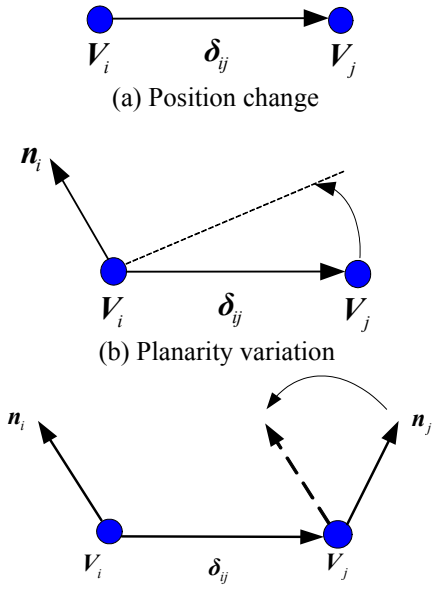

Fig. 1. Illustration of geometric information gain

3 Fuzzy Partitioning of Geometric Information Gain

According to fuzzy set theory, a geometric information gain can be deemed to a fuzzy event. The range of geometric information gain is partitioned into three intervals corresponding to weak, moderate, and strong cases of the geometric information gain in which triangular membership functions are employed to determine the membership grade for each geometric information gain value, as illustrated in Fig. 2.

Suppose that the underlying fuzzy domain is constructed by geometric information gain values in ascending order as $\Omega=\{g_1,g_2,\cdots g_{med},\cdots,g_N\}$, where g_{med} is the median value of Ω, and N is the number of total geometric information gain values. The fuzzy sets indicating weak, moderate, and strong cases of the geometric information gain are denoted by Ω_A, Ω_B and Ω_c. Membership functions corresponding to Ω_A, Ω_B and Ω_c are designed as [34]

$$\mu_A(g)=\begin{cases}1, & g \le g_{th1}\\ \dfrac{g_{med}-g}{g_{med}-g_{th1}}, & g_{th1} < g \le g_{med}\\ 0, & \text{others}\end{cases}, \tag{8}$$

$$\mu_B(g)=\begin{cases}\dfrac{g-g_{th1}}{g_{med}-g_{th1}}, & g_{th1} < g \le g_{med}\\ \dfrac{g_{th2}-g}{g_{th2}-g_{med}}, & g_{med} < g \le g_{th2}\\ 0, & \text{others}\end{cases}, \tag{9}$$

$$\mu_c(g)=\begin{cases}1, & g_{th2} < g\\ \dfrac{g-g_{med}}{g_{th2}-g_{\text{avg}}}, & g_{med} < g \le g_{th2}\\ 0, & g < g_{med}\end{cases}, \tag{10}$$

where $g \in \Omega$, are the thresholds of fuzzy sets Ω_A, Ω_B and Ω_c.

Fuzzy entropy [35] is introduced to measure the fuzziness of the presented partition as follows:

$$H(\Omega_A,\Omega_B,\Omega_C)=-\sum_{i=1}^{N}[\,h(\mu_A(g_i))+h(\mu_B(g_i))+h(\mu_C(g_i))\,], \tag{11}$$

where

$$h(\mu(g_i))=\begin{cases}-(1-\mu(g_i))\log(1-\mu(g_i))\\ \quad -\mu(g_i)\log\mu(g_i), \ \mu(g_i)\in(0,1)\\ 0, \quad \mu(g_i)=0 \text{ or } 1\end{cases}. \tag{12}$$

In (12), $\mu(g_i)$ is one of the membership function ranging at $g=g_i$. Optimal thresholds can be obtained by solving the following optimizing problem.

$$\min_{g_{th1},\,g_{th2}} H(\Omega_A,\Omega_B,\Omega_C) \tag{13}$$

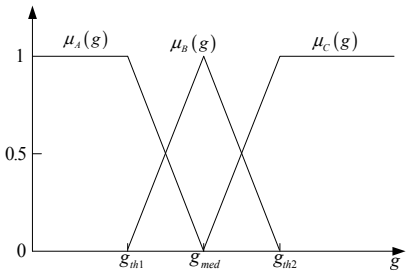

Fig. 2. Membership functions for evaluating the membership grade of each value of the geometric information gain.

Notice that there are only two thresholds regarding the fuzzy sets to be determined (Ref. Fig. 2). The fuzzy partition of Ω is equivalent to a fuzzy 2-partition [36] with a minimum fuzzy entropy. It is feasible to apply enumerated search in finding the optimal thresholds of g_{th1} and g_{th2}. Below is the algorithm description:

Step 1. According to (7), compute the values of geometric information gain for all vertices and then sort the computed results in ascending order to form Ω with g_{med} located at its center.

Step 2. Initialize the minimal fuzzy entropy H_{min} as the computed result of $H(\Omega_A,\Omega_B,\Omega_C)$ in the case of $g_{th1}=g_1$, $g_{th2}=g_{med+1}$.

Step 3. Perform the search procedure to find the optimal g_{th1} and g_{th2}:

for $th1=1$ to $med-1$

for $th2=med+1$ to N

ⅰ) For the known g_{th1} and g_{th2}, compute new membership functions $\mu_A(g)$, $\mu_B(g)$ and $\mu_C(g)$ according to (8), (9) and (10), for $g \in \Omega$.

ⅱ) Compute the fuzzy entropy of the partition of Ω using g_{th1} and g_{th2} according to (11).

ⅲ) Determine wheteher $H(\Omega_A, \Omega_B, \Omega_C)$ is less than H_{min}; if $H(\Omega_A, \Omega_B, \Omega_C) < H_{\min}$ holds, Update H_{min} with the computed value of $H(\Omega_A, \Omega_B, \Omega_C)$ at present.

end for $th2$

end for $th1$

Step 4. Use the return values of $th1$ and $th2$ from the previous step to obtain optimal g_{th1} and g_{th2}, denoted by g_{th1_opt} and g_{th2_opt}.

Step 5. Partition Ω into fuzzy sets $\{g_1, g_2, \cdots, g_{med}\}$, $\{g_{th1\_opt}, g_{th1\_opt+1}, \cdots, g_{th2\_opt}\}$ and $\{g_{med}, g_{med+1}, \cdots, g_N\}$.

4 Fundamental Edge Collapse Operation

Edge collapse operation [32] is designated to delete a vertex such as $\boldsymbol{V}_1$ or $\boldsymbol{V}_2$ and all the elements (i.e. edges and faces) around the edge, $E(\boldsymbol{V}_1, \boldsymbol{V}_2)$, and to retriangulate the remaining elements, as demonstrated in Fig. 3.

Quadric error metric is currently employed to measure the cost of a collapse during a given iteration. To do this, by associating a symmetric 4×4 matrix $\boldsymbol{Q}$ with each vertex, the error at vertex $\boldsymbol{V}_i = [x, y, z, 1]^{\mathrm{T}}$ is defined as the quadric form $\Delta(\boldsymbol{V}_i) = \boldsymbol{V}_i^{\mathrm{T}} \boldsymbol{Q} \boldsymbol{V}_i$. For a given collapse $E(\boldsymbol{V}_1, \boldsymbol{V}_2) \to \boldsymbol{V}$, a new matrix $\boldsymbol{Q}$, which approximates the error at $\boldsymbol{V}$ is calculated by a simple addition, $\boldsymbol{Q} = \boldsymbol{Q}_1 + \boldsymbol{Q}_2$. The optimal position for $\boldsymbol{V}$ can be derived by minimizing $\Delta(\boldsymbol{V})$.This is equivalent to solving equations $\partial\Delta/\partial x = \partial\Delta/\partial y = \partial\Delta/\partial z = 0$.

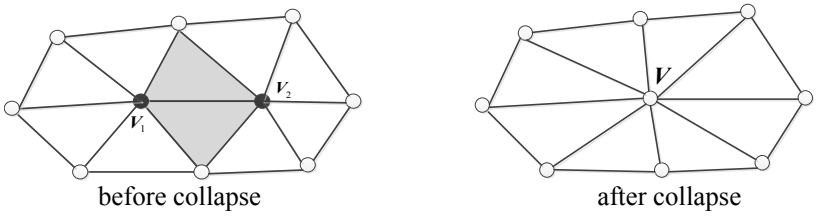

Fig. 3. Fundamental edge collapse operation

In Fig.3, the edge $E(\boldsymbol{V}_1, \boldsymbol{V}_2)$ is collapsed into a single point $\boldsymbol{V}$. As a result, the shaded triangles become degenerate and are removed during the collapse.

5 Modified Simplification Algorithm

The proposed simplification algorithm in this paper is built on egde collapsing operation and geometric information gain metric, which is partitioned by fuzzy rules. The edge collapsing cost and the position of a newly generated vertex depend on both the distances from a vertex to its neighbours and the local geometric constraints. Since the introduction of geometric information gain metric is aiming at measuring the geometric variation of local surface instead of the vertex error, the edge collapsing operation for a planar region or a region of less curvature is prior to that for a region of drastic variations in curvature. As a result, the newly generated vertices are intensively distributed in the regions of lower geometric information gain values. The modified simplification algorithm is described in detail as follows.

Step 1. Compute the geometric information gain metrics for all the initial vertices and sort them into a numerical order with the maximum at the front.

Step 2. Compute the fundamental error quadric $\boldsymbol{K}_v$ for each triangulated mesh of the original mannequin.

Step 3. Associate a certain set of triangulated planes with their concurrent vertex. Then calculate the vertex error matrix with respect to this set by summing up all the corresponding fundamental error quadrics $\boldsymbol{K}_v$'s.

Step 4. According to (13), perform fuzzy partition to yield three fuzzy sets corresponding to weak, moderate, and strong cases of the geometric information gain respectively

Step 5. Select all valid vertex pairs just among the vertices of less geometric information gain metrics in the relevant fuzzy set. For each selected pair (V_i, V_j), determine a new matrix $\bar{Q}$ which approximates the error at $\bar{V}$ by simply choosing to use the additive rule $\bar{Q} = Q_i + Q_j$.

Step 6. Compute the contraction cost $\bar{V}^T \bar{Q} \bar{V}$ of vertex pair (V_i, V_j) and put all the selected pairs in a heap keyed on cost with the minimum cost pair at the top.

Step 7. Contract the pair (V_i, V_j) of least cost from the heap to obtain a newly emerged vertex $\bar{V}$.

Step 8. Search the vertices adjacent to both V_i and V_j, which are denoted by P_1 and P_2 (only one vertex adjacent to both V_i and V_j in the case of boundary edge).

Step 9. If the geometric information gain of a newly emerged vertex $\bar{V}$ is larger than the threshold, undo any collapse operations for edges involving the new vertex $\bar{V}$; otherwise, update the costs of all valid edges involving the new vertex $\bar{V}$ followed by the collapse operation.

Step 10. Under the circumstance that the geometric information gain of P_1 is equivalent to the threshold, check whether one among the edges set involving P_1 satisfies the least error. If a certain edge is in according with the least cost error, perform collapse operation on it. The same consideration is applied to P_2.

Step 11. Iteratively proceed this process from step 1 to step 10 until the desired simplification ratio is met

6 Simulation Experiments

To compare the simplification results obtained using the fuzzy partition of geometric information gain metric based algorithm with those using Garland's algorithm, three mannequins are presented in this paper which are a Chinese adult obese woman (#1), a Chinese adult thin woman (#2) and a Chinese adult obese man (#3), as shown in Fig. 4. The adult obese woman model is with the mesh size of 23310 triangles. The adult thin woman model is with the mesh size of 6542 triangles. The adult obese man model is with the mesh size of 13052 triangles

Starting from the simplification process, it is essential to select appropriate thresholds of geometric information gain metric for the fuzzy sets. This can be obtained by resolving the optimization problem of (13). Results of optimal thresholds t_1 and t_2 are listed in Table 1.

Table 1. Optimal thresholds t_1 and t_2 of the fuzzy sets.

Mannequin	#1	#2	#3
t_1	0.0000124	0.001699	0.0000136
t_2	0.02705	0.1046	0.01078

In order to explore the simplification effect, experiments are conducted on various simplification ratios (SRs), which are defined as the ratios between the deleted mesh size and the initial mesh size. Fig. 5 has shown simplified results for the #1 mannequin. Quite a number of contour features regarding neck girth, armpit girth, waist girth, hip girth, and crotch girth are kept by geometric information gain metric. Fig. 6 has shown simplified results for the #2 mannequin. Some feature points on the female torso such as shoulder points, front neck point, bust points, armpits and crotch point are well preserved by geometric information gain metric even at high simplification ratios. Fig. 7 has shown simplified results for the #3 mannequin. Geometric information gain metric well reserve more male body shape features such as head, neck, shoulder line, belly, waist, mid-waist during the progressive simplification process.

To evaluate the quality of approximations generated by the algorithm proposed in this paper, two criteria termed maximum error $e_{\max}$ and mean squared error e_{ms} between simplified and original model are introduced as [37]:

$$e_{\max}(\mathcal{S}, \tilde{\mathcal{S}}) = \max\left(\max_{v \in \mathcal{S}} \mathcal{D}_v(\tilde{\mathcal{S}}), \max_{v \in \tilde{\mathcal{S}}} \mathcal{D}_v(\mathcal{S})\right), \tag{14}$$

$$e_{ms}(\mathcal{S}, \tilde{\mathcal{S}}) = \frac{1}{M + \tilde{M}}\left(\sum_{v \in \mathcal{S}} \mathcal{D}_v^2(\tilde{\mathcal{S}}) + \sum_{v \in \tilde{\mathcal{S}}} \mathcal{D}_v^2(\mathcal{S})\right). \tag{15}$$

In (12) and (13), M and $\tilde{M}$ are the numbers of vertices corresponding to the original and the simplified models $\mathcal{S}$ and $\tilde{\mathcal{S}}$, and distance $\mathcal{D}_v(\mathcal{S}) = \min_{p \in \mathcal{S}} \|v - p\|$ is the minimum distance from v to the closest facet of $\mathcal{S}$.

Resulting errors of the simplification using fuzzy partitioning of geometric information gain metric are compared to those using Garland's metric, which are detailed in the Tables 2, 3, and 4.

(a) (b) (c)

Fig. 4. Initial mannequin: (a) a Chinese adult obese woman #1, (b) a Chinese adult thin woman #2 and (c) a Chinese adult obese man #3.

(a) (b) (c)

Fig. 5. Simplified results for the mannequin #1: (a) SR=30%, (b) SR=50% and (c) SR=90%.

(a) (b) (c)

Fig. 6. Simplified results for the mannequin #2: (a) SR=30%, (b) SR=50% and (c) SR=90%.

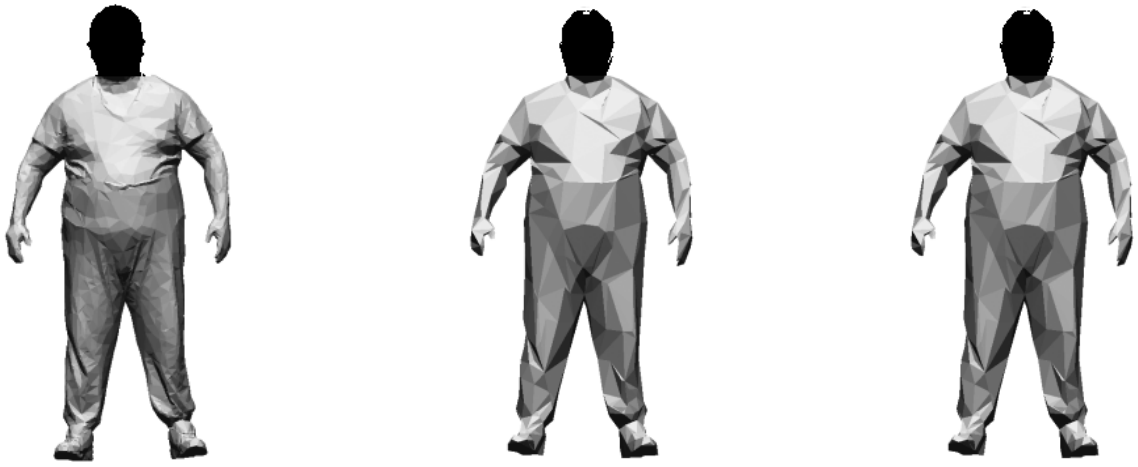

(a) (b) (c)

Fig. 7. Simplified results for the mannequin #3: (a) SR=30%, (b) SR=50% and (c) SR=90%.

Table 2. Comparison of the simplification errors of mannequin #1

SR	Garland's Algorithm		Algorithm of this paper	
	$e_{\max}$	e_{ms}	$e_{\max}$	e_{ms}
10%	0.02856	0.000004	0.02337	0.000004
20%	0.04493	0.000013	0.0294	0.000012
30%	0.04493	0.000026	0.03147	0.000024
40%	0.04493	0.0000 45	0.04493	0.000044
50%	0.04802	0.000077	0.04493	0.000074
60%	0.05831	0.000133	0.0535	0.000128
70%	0.05926	0.000243	0.05926	0.000246
80%	0.07613	0.000544	0.06181	0.000532
90%	0.09306	0.002081	0.07721	0.00204

Table 3. Comparison of the simplification errors of mannequin #2

SR	Garland's Algorithm		Algorithm of this paper	
	$e_{\max}$	e_{ms}	$e_{\max}$	e_{ms}
10%	0.03287	0.000006	0.0319	0.000005
20%	0.04326	0.00002	0.03856	0.000022
30%	0.04452	0.000054	0.04092	0.000051
40%	0.04723	0.000107	0.04529	0.0011
50%	0.05389	0.000191	0.05139	0.000198
60%	0.06571	0.000344	0.06488	0.00035
70%	0.06691	0.000656	0.06142	0.000629
80%	0.08825	0.001495	0.07602	0.00148
90%	0.1036	0.005485	0.1006	0.005441

It can be observed that there exist measurable gaps in the simplification errors between Garland's quadric error metric algorithm and geometric information gain algorithm with fuzzy partitioning proposed in this paper. In the case of simplified results of mannequin #1, the maximum error of geometric information gain metric algorithm with fuzzy partitioning is apparently less than that of Garland's quadric error metric algorithm when the simplification ratio is either larger than 70% or less than 40%, while in the other case of simplified results of mannequin #2, both the maximum error and the mean squared error of geometric information gain algorithm with fuzzy partitioning have a certain degree of reduction in contrast with Garland's quadric error metric algorithm when the simplification ratio is larger than 10% and less than 90%. As far as mannequin #3 is concerned, the maximum error of geometric information gain algorithm with fuzzy partitioning is clearly less than that of Garland's quadric error metric algorithm when the simplification ratio is ranging from 30% to 80%, which is accompanied by a moderate reduction of the mean squared error of geometric information gain algorithm with

fuzzy partitioning relative to that of Garland's quadric error metric algorithm when the simplification ratio is ranging from 10% to 90%. According to Tables 2, 3 and 4, fuzzily partitioned geometric information gain simplification algorithm outperforms Garland's quadric error metric algorithm in the sense of maximum error. The reason is that vertices among the detailed regions on the object surface are progressively maintained rather than contracted in the course of simplification guided by the geometric information gain metric.

Table 4. Comparison of the simplification errors of mannequin #3

SR	Garland's Algorithm		Algorithm of this paper	
	$e_{\max}$	e_{ms}	$e_{\max}$	e_{ms}
10%	0.0295	0.000005	0.0295	0.000005
20%	0.04396	0.000021	0.04396	0.000021
30%	0.05233	0.000046	0.04135	0.000004
40%	0.06285	0.0000 87	0.05233	0.000088
50%	0.0868	0.000161	0.06359	0.000144
60%	0.09281	0.000302	0.0788	0.000261
70%	0.09281	0.000549	0.08196	0.000547
80%	0.1029	0.0012	0.08476	0.000104
90%	0.108	0.00409	0.119	0.00401

7 Conclusions

In this paper, a new mesh simplification method for mannequins based on geometric information gain has been presented, which is a function of distance, non-planarity, change of the normals. The newly presented method is characterized by a number of aspects such as the partition trick of geometric information gain metric, the simplification strategy, the error evaluation criteria and the capability to preserve mesh characteristics. Due to introduction of geometric information gain metric, the edge contraction cost as well as the optimal position of new vertex are determined not only by the distance but also by the shape variation on the mannequin surface. There is a distinct difference of the edge contraction cost between the high convature region and the low convature region. As a result, the edge collapse operation is performed on the low convature region prior to the high convature through fuzzily partitioning the geometric information gain values. The position of newly resulted vertex is much close to triangulated meshes with high degree geometric information gain metrics.

Simulation experiments have been run on a set of mannequins involving a chinese adult obese woman, a chinese adult thin woman and a chinese adult obese man. Results obtained by the proposed method in this paper are compared to the results with Garland's quadric error metric algorithm. From the geometric fidelity view of point, the proposed simplification approach produces better results than the quadric error metric based simplification approach in terms of maximum error, which would constitute a promising way to applications of garment industry.

Acknowledgement

This work was supported by the Scientific Research Key Program of Beijing Municipal Commission of Education under Grant No. KZ201210012014 and by the training program of the Scientific research plan of Beijing Institute of Fashion Technology under Grant No. 2014AL-06.

References

[1] http://www.tc2.com/index_3dbodyscan.html.

[2] http://www.vitronic.de/en/industry- logistics/sectors/other-industries/3d-bodyscanner.html

[3] http://www.creaform3d.com/zh

[4] http://www.3dcamega.com/products.asp

[5] J. Rossignac, P. Borrel, "Multi-resolution 3D approximation for rendering complex scenes," in *Geometric Modeling in Computer Graphics*, pp. 455-465, 1993.

[6] K. L. Low, T. S. Tan, "Model simplification using vertex clustering," in *Proceedings of 1997 Symposium on Interactive 3D Graphics*, pp. 75-82, 1997.

[7] P. Lindstrom, "Out-of-core simplification of large polygonal models," in *Proceedings of the SIGGRAPH 2000*, pp.259-262, 2000.

[8] A. D. Kalvin, R. H. Taylor, "Superfaces: polygonal mesh simplification with bounded error," *IEEE Computer Graphics and Applications*, Vol. 16, No. 3, pp. 64-77, 1996.

[9] J. Li, Z. Tang, "An improved greedy algorithm for simplification of triangular meshes," in *Proceedings of CAD & Graphics'97*, pp. 119-122, 1997.

[10] P. Hinker, C. Hansen, "Geometric optimization," in *Proceedings of the IEEE Visualization'93*, pp.189-195, 1993.

[11] J. Cohen, A. Varshney, D. Manocha, et al., "Simplification envelopes," in *Proceedings of the SIGGRAPH'96*, pp. 119-128, 1996.

[12] G. Turk, "Re-tiling polygonal surfaces," in *Proceedings of the SIGGRAPH'92*, pp. 52-64, 1992.

[13] T. He, L. Hong, A. Kaufman, et al., "Voxel based object simplification," in *Proceedings of the 1995 IEEE Conference on Visualization (Visualization'95)*, pp. 296-303, 1995.

[14] T. He, L. Hong, A. Varshney, et al., "Controlled topology simplification," *IEEE Transactions on Visualization and Computer Graphics*, Vol. 2, No. 2, pp. 171-184, 1996.

[15] W. J. Schroeder, J. A. Zarge, and W. E. Lorensen, "Decimation of triangle meshes," In *Proceedings of the SIGGRAPH'92*, pp. 65-70, 1992.

[16] H. Hoppe, T. DeRose, T. Duchamp, et al., "Mesh optimization," in *Proceedings of the SIGGRAPH'93*, pp. 19-26, 1993.

[17] B. Hamann, "A data reduction scheme for triangulated surface," *Computer Aided Geometric Design*, Vol. 11, No. 2, pp. 197-214, 1994.

[18] P. Castelló, M. Sbert, M. Chover, et al., "Viewpoint entropy-driven simplification," in *Proceedings of the WSGG 2007*, pp.249-256, 2007.

[19] P. Castelló, M. Sbert, M. Chover, et al., "Viewpoint-driven simplification using mutual information," *Computers & Graphics*, Vol. 32, pp. 451-463, 2008.

[20] P. Castelló, M. Sbert, M. Chover, et al., "Viewpoint-based simplification using f-divergences," *Information Sciences*, Vol. 178, pp. 2375-2388, 2008.

[21] P. Lindstrom, G. Turk, "Image-driven simplification," ACM Transactions on Graphics, Vol.19, No.3, pp.204-241, 2000.

[22] E. Zhang, G. Turk, "Visibility-guided simplification," in *Proceedings of IEEE Visualization 2002*, Vol. 31, pp. 267-274, 2002.

[23] C. H. Lee, A. Varshney, D.W. Jacobs, "Mesh saliency," *ACM Transactions on Graphics*, Vol. 24, No. 3, pp. 659-666, 2005.

[24] D. Xiaohui, Y. Baocai, K. Dehui, "Triangle mesh simplification algorithm based on edge collapse," *Computer Engineering*, Vol. 33, No. 12, pp. 12-15, 2007. (in Chinese)

[25] W. Fang, C. Wenjing, Z. Haitao, "Research of simplification algorithm for modeling based on normal important degree of triangular facets," *Computer & Digital Engineering*, Vol. 39, No. 7, pp. 6-8, 100, 2011. (in Chinese)

[26] M. Soucy, D. Laurendeau, "Multiresolution surface modeling based on hierarchical triangulation," *Computer Vision and Image Understanding*, Vol. 63, No. 1, pp.1-14, 1996.

[27] M. Alexa, J. Behr, D. Cohen-Or, et al., "Point set surfaces," in *Proceedings of 12th IEEE Visualization 2001 (VIS 2001)*, pp.21-28, 2001.

[28] M.E. Algorri, F. Schmitt, "Mesh simplification," Computer Graphics Forum, Vol. 15, No. 3, pp. 77–86, 1996.

[29] R. Ronfard, J. Rossignac, "Full-range approximation of triangulated polyhedra," *Computer Graphics Forum*, Vol. 15, No. 3, pp. 67–76, 1996.

[30] H. Hoppe, "Progressive meshes," in *Proceedings of the SIGGRAPH'96*, pp. 99-108, 1996.

[31] H. Hoppe, "View-dependent refinement of progressive meshes," in *Proceedings of the SIGGRAPH'97*, pp. 189-198, 1997.

[32] M Garland, P.S. Heckbert, "Surface simplification using quadric error metrics," in *Proceedings of SIGGRAPH'97*, pp. 209-216,1997.

[33] R. Szeliski, D. Tonnesen, "Surface modeling with oriented particle systems," in *Proceedings of SIGGRAPH'92*, Vol. 26, No.4, pp. 185-194, 1992.

[34] Z. Yunjie, *Research of Image Segmentation Methods Based on Fuzzy Systems Theory*, Ph.D. Thesis, Dalian Maritime University, 2007.

[35] A. De Luea, S. Termini, "A Definition of a nonprobabilistic entropy in the setting of fuzzy sets theory," *Information and Control*, Vol. 20, pp. 301-312, 1972.

[36] H. D. Cheng, J. Chen, J. Li, "Threshold selection based on fuzzy," *Pattern Recognition*, Vol. 31, No.7, pp. 857-870, 1998.

[37] M.Garland, *Quadric-Based Polygonal Surface Simplification*, Ph. D. Thesis, Carnegie Mellon University, 1999.